# INFLUENCE OF MILLING TIME ON THE MICROSTRUCTURE OF IMMISCIBLE Cu-Fe-Co-W ALLOY PREPARED BY POWDER METALLURGY

Ondřej ADAM, Vít JAN

*Brno University of Technology, Faculty of Mechanical Engineering, Brno, Czech Republic, EU,*
*Ondrej.Adam@vutbr.cz*

https://doi.org/10.37904/metal.2020.3613

**Abstract**

The immiscible Cu-Fe system is often used as a base for new advanced alloys. In the current study, three batches of the same immiscible $(Cu_{70}Fe_{15}Co_{15})_{89}W_{11}$ alloy were prepared by mechanical alloying with different milling time and subsequent SPS consolidation. The effect of milling time on the microstructure and the properties of the powder and bulk samples was subject to study. The microstructure of the milled powder samples consists of FCC Cu-based supersaturated solid solution and particles of pure W, which did dissolve only partially. During the SPS consolidation, Cu-based supersaturated solid solution partially decomposed and (Fe, Co)-based solid solution, $(Fe, Co)_7W_6$ phase, and pure Cu phase were formed. Increasing the milling time results in the finer microstructure of the consolidated samples and in the enhancement of their hardness. The maximum hardness achieved is 395HV1. The longer milling time has a negative effect of decrease in relative density of consolidated samples, caused by larger size of the milled powders.

**Keywords:** Immiscible alloy, mechanical alloying, phase separation, spark plasma sintering

## 1. INTRODUCTION

Most alloys are formed in systems with a negative enthalpy of mixing which leads to the formation of solid solutions and intermetallic compounds [1]. There are, however, many systems that do not form alloys at room temperature due to their positive enthalpy of mixing [2,3]. In this case, elements show no mutual solubility at room temperature and, therefore, the equilibrium microstructure is composed of separated phases of two pure elements. This allows preparing materials with an interesting combination of properties such as high strength and high electrical conductivity or superior magnetic properties [4-7] that is difficult to achieve with common materials. In addition, it is possible to alloy a selected phase by elements miscible with one of the basic components and immiscible with the second one, which allows control the resulting microstructure and tailor the mechanical properties [8-10]. Nevertheless, most immiscible systems exhibit miscibility gap even in the liquid state, which leads to the effect of liquid separation and, therefore, it is very difficult to prepare immiscible alloys with a uniform microstructure by means of conventional casting. Various methods such as gas atomization, high pressure torsion, laser melting technique, or mechanical alloying have been thus experimentally proven to be feasible for fabrication immiscible alloys [4,11-13].

The Cu-Fe is a well-known immiscible alloy with low positive enthalpy of mixing showing metastable miscibility gap in the liquid state. Cu-Fe alloy is being studied intensively due to its great combination of high electrical conductivity and good mechanical strength that makes it a promising material for sensors, electrical contact materials etc [5,14]. Moreover, this system is used as a base for new advanced alloys [8,9,15]. At room temperature, the microstructure of Cu-Fe alloy consists of separated BCC-Fe phase and FCC-Cu phase. This allows alloying each of the phases individually and creating hierarchical material with desirable microstructure and mechanical properties. Elements such as Co, Si, Nb, W, etc. are added to Cu-Fe alloy in order to fabricate high strength immiscible material [8,9,16]. To achieve optimal strength-ductility combination, it is essential to

understand the influence of additive elements on the resulting microstructure and to optimize methods of fabrication.

Mechanical alloying has been proven to be a suitable method for the preparation of Cu-based immiscible alloy [6,17]. This method, however, has many variable parameters that strongly influence the properties of the resulting powder. One of the most important parameters is the milling time that has a significant effect on the size and homogeneity of the powder. In this paper, three different milling times were used for the preparation of immiscible $(Cu_{70}Fe_{15}Co_{15})_{89}W_{11}$ alloy and the final powder size and its microstructure were investigated. Subsequently, the samples were consolidated by spark plasma sintering technique, and the observation of microstructural evolution was carried out. Furthermore, Vickers hardness and relative density of samples were measured.

## 2. MATERIALS AND METHODS

Immiscible alloy with the chemical composition of $(Cu_{70}Fe_{15}Co_{15})_{89}W_{11}$ was prepared by powder metallurgy route. Elemental powders of iron, cobalt, copper, and tungsten with a purity of 99.5% were used as starting materials. The powder mixture was entered into milling bowl together with hardened bearing steel balls of 10 mm and 15 mm diameters, in a 1:10 powder-to-ball weight ratio (PBR). Mechanical alloying was performed under argon atmosphere in a planetary ball mill (Fritsch Pulverisette 6) with the milling speed of 240 RPM. The powders were milled for 15 h, 50 h, and 100 h (referred to as W15, W50, and W100, respectively). Each milling comprised of cycles that were set as 60 min of milling and 30 min idle time. To remove the powder stuck to the surfaces of the milling balls, an additional 15 min of wet milling in ethanol was performed.

The milled powders were consolidated by spark plasma sintering technology (SPS) using Sumitomo Coal Mining, Dr. Sinter SPS machine in Central European Institute of Technology in Brno (CEITEC). Consolidation was carried out in a vacuum atmosphere using graphite die with 20 mm inner diameter. The following sintering scheme was used: 100 °C·min$^{-1}$ heating rate from RT up to 600 °C at the pressure of 6 MPa with a 5 min dwell time at 600 °C to remove any organic compound potentially present. Then, 100 °C·min$^{-1}$ from 600 °C up to 800 °C with a 5 min dwell time at 800 °C and the pressure of 50 MPa. After sintering, the samples were spontaneously cooled down to room temperature in a vacuum atmosphere. The resulting bulk samples were cylinders approximately 6 mm high with 20 mm diameter.

Powder and bulk samples for microstructural observations were prepared by hot mounting in a polymeric resin and grinding with SiC paper up to 4000 grit size, followed by polishing with 3 μm and 1 μm particle size diamond paste. The phase composition and crystallite size of phases were measured by X-ray diffraction (XRD). Philips X'Pert Pro diffractometer was used with Cu-K$\alpha$ radiation($\lambda$ = 0.15418 nm), operated at 40 kV voltage with a current of 30 mA. A continuous scanning was performed for 2$\theta$from 20° to 120° by the speed of 0.014°·min$^{-1}$ and step size of 0.0167°. The scanning electron microscope (SEM) characterization was performed using ZEISS Ultra Plus FEG microscope. Energy-dispersive X-ray spectroscopy (Aztec, Oxford Instruments) (EDS) was used for the measurement of chemical composition.

The Vickers hardness was measured using Qness Q10A hardness tester with 1000 g load and 10 s dwell time. The presented values are an average of six measurements. Relative density was measured on the cross-section of the samples at 100× magnification by image analysis.

To obtain an equilibrium phase diagram of the present alloy, CALPHAD calculations were performed using ThermoCalc software (version 2020a) with thermodynamic database TCHEA3 v3.1.

## 3. RESULTS AND DISCUSSION

**Figure 1** shows the equilibrium phase diagram of the $Cu_{70}Fe_{15}Co_{15}$ alloy with varying W contents. Up to 890°C the structure is predicted as FCC pure Cu, BCC (Fe, Co)-based solid solution and rhombohedral intermetallic

phase (Fe, Co)$_7$W$_6$. It is expected that the structure of milled powders will not correspond to the calculated phase diagram, as mechanical alloying is a non-equilibrium fabrication technique. However, the alloy should reduce its Gibbs energy during sintering and, therefore, moves its phase composition towards an equilibrium state.

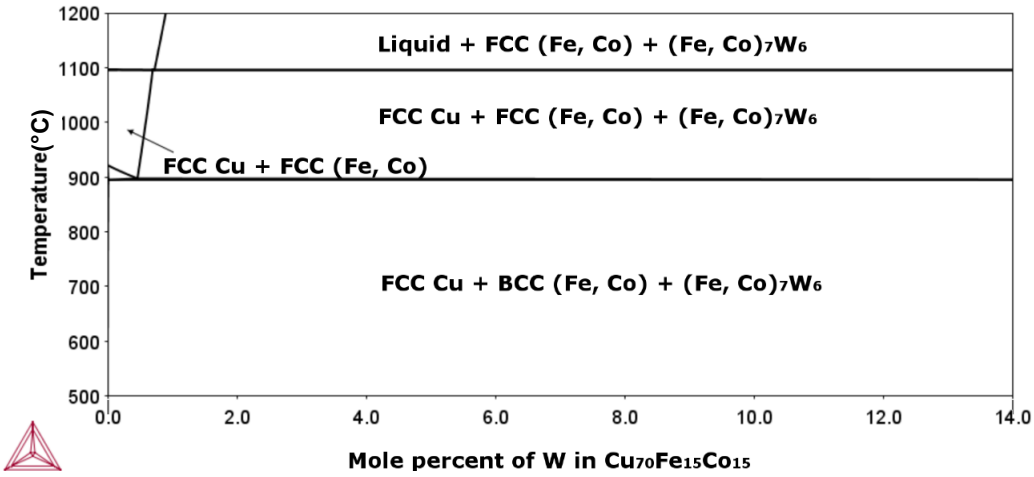


**Figure 1** Equilibrium phase diagram of $Cu_{70}Fe_{15}Co_{15}$-W system

### 3.1. Powder samples

The size of milled powder increases with increasing milling time (**Table 1**). The cause for this is the excessive cold welding effect, which typically happens upon dry milling of ductile metals and their alloys such as Sn, Al, or Cu [18]. The XRD analysis of the milled powders presents that the microstructure is composed of two phases: a FCC phase, corresponding to Cu-based supersaturated solid solution of all elements, and a BCC phase, corresponding to pure W. Crystallite size and weight fraction of both phases are presented in **Table 1**. The smallest crystallite sizes were achieved in W50 sample. Presumably, sample W100 is partially recrystallized due to high energy input upon milling which leads to increase in the crystallite sizes of both phases. In **Figure 2**, the SEM micrographs of the milled powders are shown. The microstructure of sample W15 contains relatively large W particles, compared to the other two samples (**Figure 1(a)**). The weight fraction of pure W analyzed in the microstructure is 28.8 % that is the same as the weight fraction of original W powder which means that no W dissolved into Cu-based solid solution. Tungsten particles in the microstructure are therefore only milled particles of the original W powder. Microstructures of W50 and W100 samples are very similar, containing round nano-sized W particles and several voids (**Figure 1(b, c)**). In both samples, the weight fraction of pure W particles is about 10% lower than in sample W15 (**Table 1**). Tungsten was, therefore, partially dissolved into Cu-based supersaturated solid solution by mechanical alloying. Since the weight fraction of pure W is almost the same in samples W50 and W100, it is possible to conclude that approximately 10 wt% of W can be maximally dissolved into Cu-based supersaturated solid solution in the $Cu_{70}Fe_{15}Co_{15}$-W system.

**Table 1** XRD analysis and powder size of milled powders

| **Samples** | **FCC** | | **BCC** | | **Particle size** (μm) |
|---|---|---|---|---|---|
| | **Amount** (wt%) | **Crystallite size** (nm) | **Amount** (wt%) | **Crystallite size** (nm) | |
| W15 | 71.2 | 12.2 | 28.8 | 25.3 | 88 |
| W50 | 81.9 | 11.9 | 18.1 | 18.6 | 290 |
| W100 | 80.4 | 14.4 | 18.6 | 19.5 | 434 |

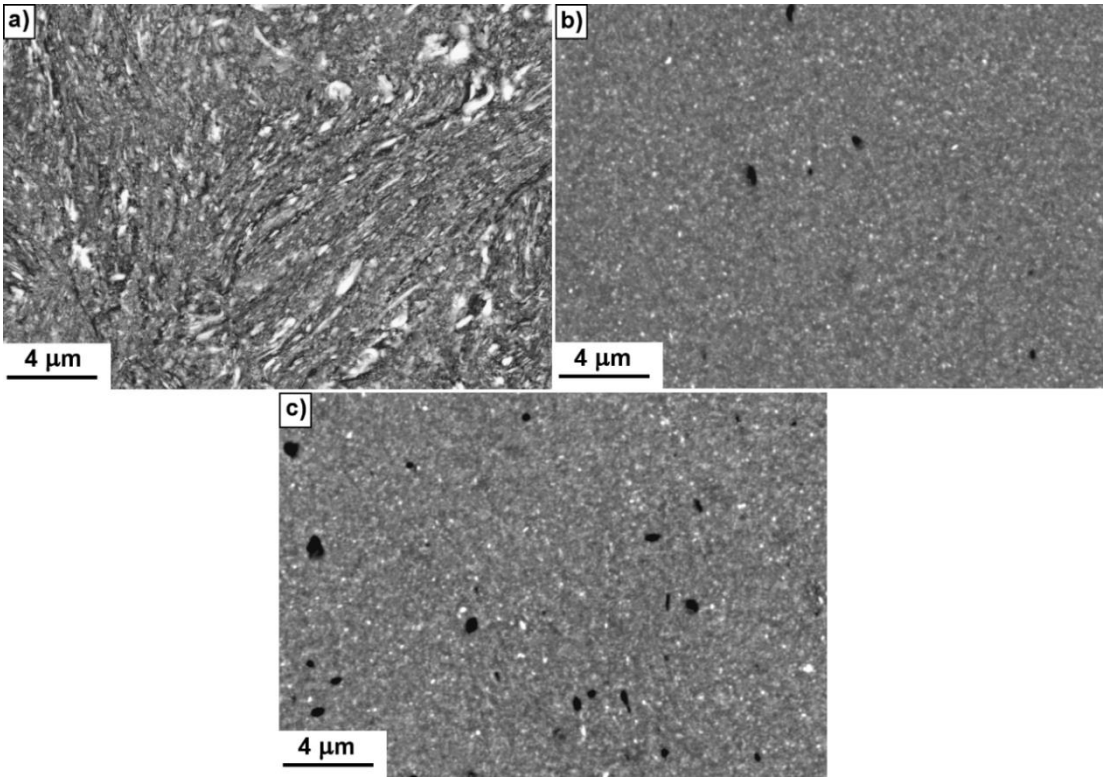


**Figure 2** Micrographs of milled powders: a) W15; b) W50; c) W100

### 3.2. Bulk samples

According to XRD analysis (**Table 2**), the microstructure of consolidated samples is composed of FCC Cu-based phase, BCC (Fe, Co)-rich phase, and (Fe, Co)$_7$W$_6$ phase, which is in good agreement with the equilibrium phase diagram. Nevertheless, the equilibrium amount of FCC phase is 53.1 wt% which means, that only partial decomposition of Cu-based supersaturated solid solution occurred during sintering and, therefore, the amount of FCC phase measured by XRD corresponds to the sum of the amounts of Cu-based supersaturated solid solution and Cu phase. The reason for this incomplete decomposition is the short SPS procedure time. In **Figure 3**, the SEM micrographs of the consolidated samples are shown. Microstructures of all samples contain large areas of pure Cu that have been formed by decomposition and fine mixture of (Fe, Co)$_7$W$_6$ phase, (Fe, Co)-rich phase, and Cu-based supersaturated solid solution. It is not possible to identify (Fe, Co)-rich phase and Cu-based supersaturated solid solution due to an extremely slight difference in contrast which is caused by the presence of (Fe, Co)$_7$W$_6$ phase. In addition, except for the phase of pure Cu, the chemical composition of all other phases cannot be measured by EDS since the size of the phases is below the detection limit of the EDS measurement. The average chemical composition of these phases is practically the same for all samples: 50 wt% Cu, 11 wt% Fe, 11 wt% Co, 28 wt% W.

Sample W15 possesses the lowest value of hardness, which is the result of its relatively coarse microstructure, compared to other samples (**Figure 3(a)**). Microstructures of samples W50 and W100 are very fine and uniform - see **Figure 3(b, c)** that leads to enhanced hardness (**Table 2**). Sample W100 shows higher value of hardness than sample W50 despite of lower amount of (Fe, Co)$_7$W$_6$ phase that is assumed to be the hardest phase in the present microstructure. The probable reason could be a decrease in the strengthening of Cu-based supersaturated solid solution caused by the formation of (Fe, Co)$_7$W$_6$ phase, which does not compensate this decrease in hardness. The hardness of sample W100 is approximately twice higher than the hardness of Cu-Fe alloy [19]. On the other hand, sample W100 shows the lowest relative density after consolidation whereas sample W15 is nearly fully densified (**Table 2**). The reason is the difference in the size of milled

powders (**Table 1**). The coarse powder is less suitable for consolidation. To reduce the cold welding effect, a process control agent (PCA) such as methanol, ethanol, and stearic acid is usually added to the powder mixture during milling [18, 20].

**Table 2** The proportion of phases measured by XRD, HV1 and relative density of bulk samples

| **Sample** | **Amount of phases** (wt%) | | | **Hardness HV1** | **Relative density** (%) |
|---|---|---|---|---|---|
| | **FCC** | **BCC** | **$(Fe, Co)_7W_6$** | | |
| W15 | 70.3 | 14.6 | 15.1 | 265 | 99.9 |
| W50 | 67.0 | 13.3 | 19.7 | 345 | 93.7 |
| W100 | 71.8 | 16.3 | 12.9 | 395 | 90.3 |

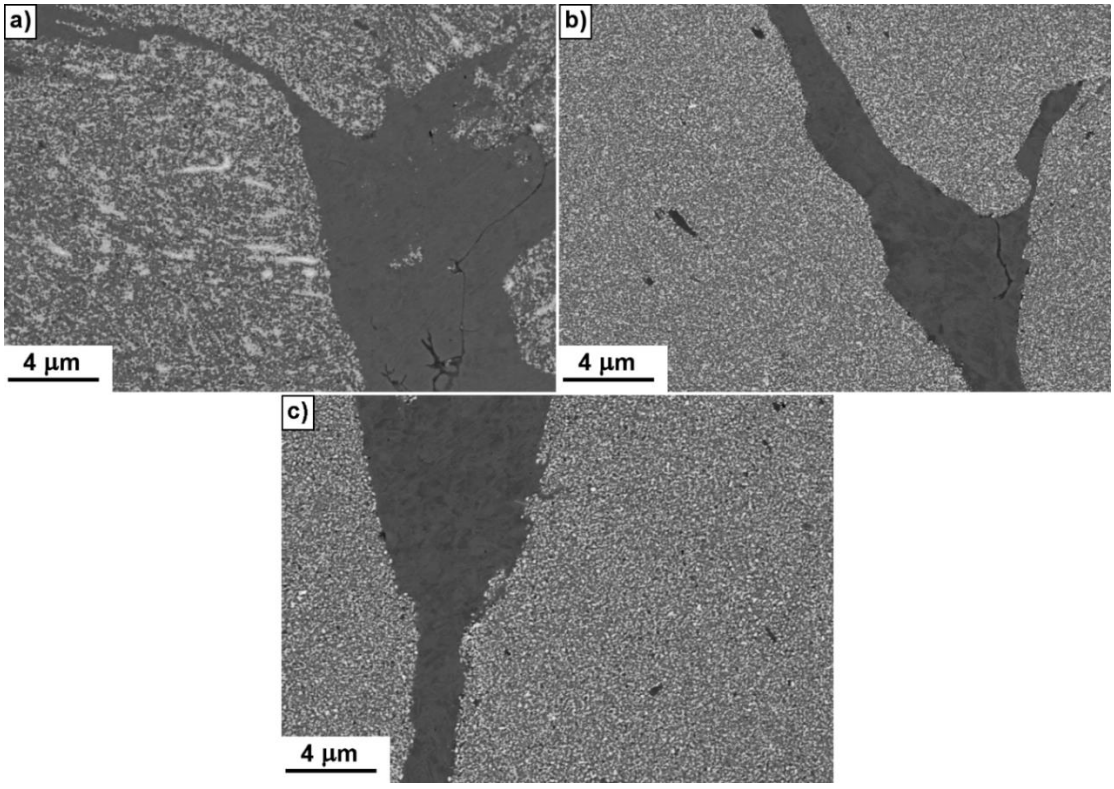


**Figure 3** Micrographs of bulk samples: a) W15; b) W50; c) W100

## 4. CONCLUSIONS

In this paper, an immiscible $(Cu_{70}Fe_{15}Co_{15})_{89}W_{11}$ alloy was prepared by powder metallurgy. Based on the results, the following conclusions can be drawn:

- size of milled powders increases with increasing milling time which causes decreasing of the relative density of the consolidated samples
- approximately 10 wt% of W can be maximally dissolved into FCC Cu-based supersaturated solid solution, that is formed during mechanical alloying
- the microstructure of consolidated samples consists of partially decomposed Cu-based supersaturated solid solution, $(Fe, Co)_7W_6$ phase, (Fe, Co)-rich solid solution and pure Cu phase; the finer microstructure was achieved with longer milling time

- increasing milling time leads to enhancement of hardness; the maximum hardness achieved is 395 HV1

## ACKNOWLEDGEMENTS

***This work was supported by the project no.FSI-S-20-6484 of BUT. The authors thank Ing. Václav Pouchlý, Ph.D. in CEITEC for helping to perform consolidation of milled powders by SPS.***

## REFERENCES

[1] CAMPBELL, F. C. *Phase diagrams: Understanding the basics.* Materials Park, Ohio: ASM International, 2012

[2] RATKE, L., DIEFENBACH, S. Liquid immiscible alloys. *Materials Science and Engineering*: R: Reports. 1995, vol. 15, no. 7-8, pp. 263-347.

[3] MA, E. Alloys created between immiscible elements. *Progress in Material Science*. 2005, vol. 50, no. 4,pp. 413-509.

[4] BOTCHAROVA, E., FREUDENBERGER, J., SCHULTZ, L. Mechanical and electrical properties of mechanically alloyed nanocrystalline Cu–Nb alloys. *Acta Materialia*. 2006, vol. 54, no. 12, pp. 3333-3341. ISSN 1359-6454.

[5] STEPANOV, N.D. Evolution of microstructure and mechanical properties in Cu–14%Fe alloy during severe cold rolling. *Materials Science and Engineering: A*. 2013, vol. 564, pp. 264-272.

[6] MONDAL, B.N. et al. Magnetic response of Cu (25wt.%)-316 grade stainless steel processed by ball milling. *Journal of Non-Crystalline Solids*. 2012, vol. 358, no. 4, pp. 810-813.

[7] LIU, S. et al. A comprehensive investigation on microstructure and magnetic properties of immiscible Cu-Fe alloys with variation of Fe content. *Materials Chemistry and Physics*. 2019, vol. 238, in print..

[8] SARKAR, S., SRIVASTAVA, C., CHATTOPADHYAY, K. Development of a new class of high strength copper alloy using immiscibility route in Cu-Fe-Si system: Evolution of hierarchical multi-scale microstructure. *Materials Science and Engineering: A*. 2018, vol. 723, pp. 38-47.

[9] JEONG, Y. et al. A study on the micro-evolution of mechanical property and microstructures in (Cu-30Fe)-2X alloys with the addition of minor alloying elements. *Journal of Alloys and Compound.* 2019, vol. 786, pp. 341-345.

[10] SUN, X. et al. Microstructure formation and electrical resistivity behavior of rapidly solidified Cu-Fe-Zr immiscible alloys. *Journal of Materials Science & Technology*. 2020, vol. 44, pp. 201-208.

[11] HE, J., ZHAO, J. Behavior of Fe-rich phase during rapid solidification of Cu–Fe hypoperitectic alloy. *Materials Science and Engineering: A*. 2005, vol. 404, no. 1-2, pp. 85-90.

[12] MOUSAVI, T. et al. Fabrication and characterization of nanostructured immiscible Cu–Ta alloys processed by high-pressure torsion. *Journal of Alloys and Compounds*. 2020, vol. 832, in print.

[13] ZHOU, S. et al. *Investigation of Cu–Fe-based coating produced on copper alloy substrate by laser induction hybrid rapid cladding*. 2014, vol. 59, pp. 131-136.

[14] GAO, H. et al. Effect of Ag on the microstructure and properties of Cu–Fe in situ composites. *Scripta Materialia*. 2005, vol. 53, no. 10, pp. 1105-1109.

[15] MOON, J. et al. A new strategy for designing immiscible medium-entropy alloys with excellent tensile properties. *Acta Materialia*. 2020, vol. 193, pp. 71-82.

[16] LIU, N. a et al. Microstructure evolution of undercooled Fe–Co–Cu alloys. *Physica B: Condensed Matter*. 2011, vol. 406, no. 4, pp. 957-962.

[17] RABIEE, M. et al. Processing of Cu-Fe and Cu-Fe-SiC nanocomposites by mechanical alloying. *Advanced Powder Technology*. 2017, vol. 28, no. 8, pp. 1882-1887.

[18] SURYANARAYANA, C. Mechanical alloying and milling. *Progress in Materials Science*. 2001, vol. 46, no. 1-2, pp. 1-184.

[19] GAO, H. et al. Effect of Ag on the aging characteristics of Cu–Fe in situ composites. *Scripta Materialia*. 2006, vol. 54, no. 11, pp. 1931-1935.

[20] FANG, Q., KANG Z. An investigation on morphology and structure of Cu–Cr alloy powders prepared by mechanical milling and alloying. *Powder Technology*. 2015, vol. 270, pp. 104-111.